www.lpr-journal.org Vol. 7 No. 3 May 2013

LASER & PHOTONICS REVIEWS

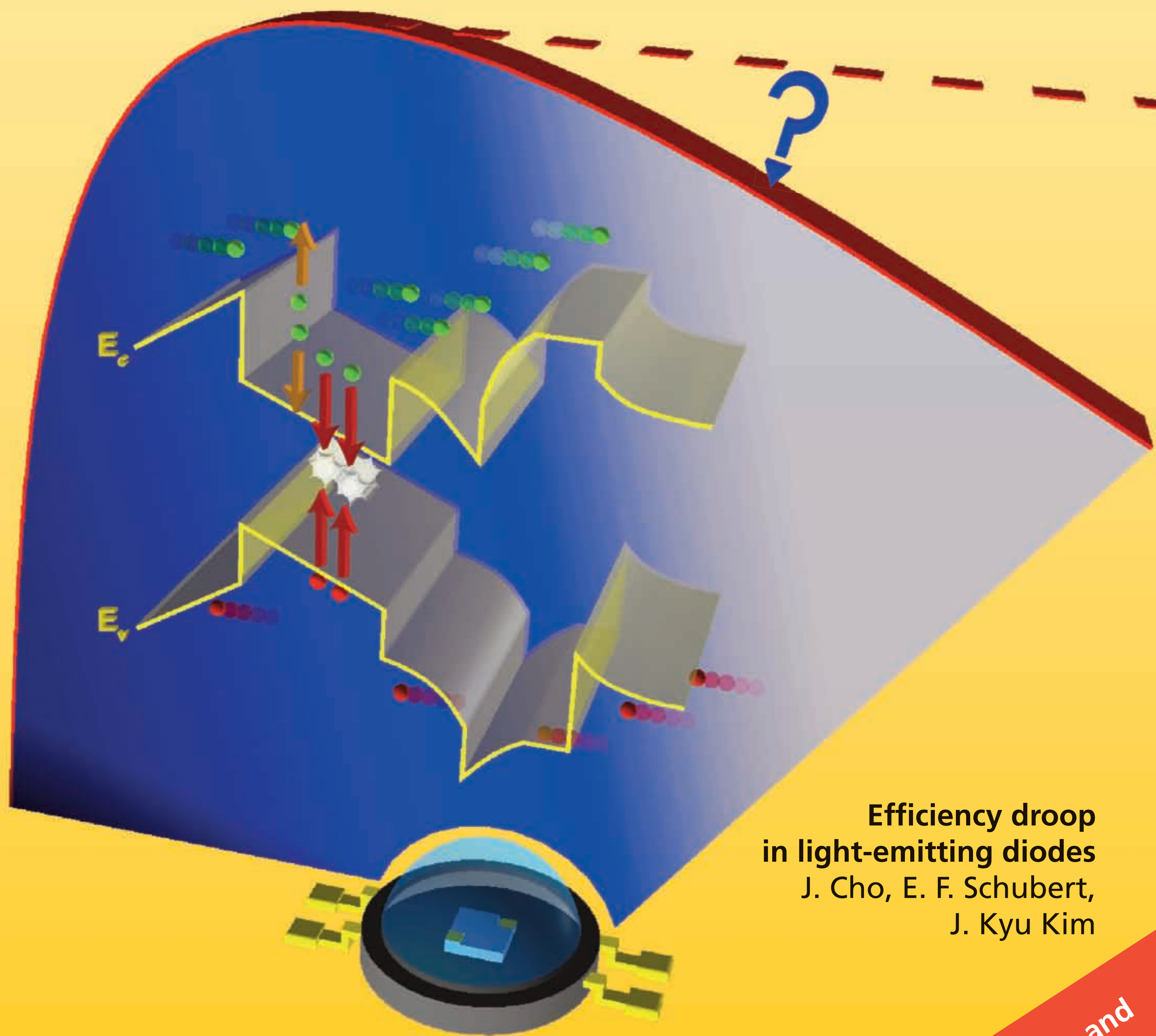

Efficiency droop in light-emitting diodes

J. Cho, E. F. Schubert, J. Kyu Kim

Now open for Letters and Original Articles

WILEY-VCH

ISSN 1863-8880 Laser Photonics Rev., Vol. 7, No. 3 (May), 303–452 (2013)

www.lpr-journal.org

LASER & PHOTONICS REVIEWS

WILEY-VCH

REPRINT

LASER & PHOTONICS REVIEWS

Laser Photonics Rev. 7, No. 3, 408–421 (2013) / DOI 10.1002/lpor.201200025

REVIEW ARTICLE

Abstract Efficiency droop, i.e. the loss of efficiency at high operating current, afflicts nitride-based light-emitting diodes (LEDs). The droop phenomenon is currently the subject of intense research, as it retards the advancement of solid-state lighting which is just starting to supplant fluorescent as well as incandescent lighting. Although the technical community does not yet have consented to a single cause of droop, this article provides a summary of the present state of droop research, reviews currently discussed droop mechanisms, and presents a recently developed theoretical model for the efficiency droop. In the theoretical model, carrier leakage out of the active region caused by the asymmetry of the pn junction, specifically the disparity between electron and hole concentrations and mobilities, is discussed in detail. The model is in agreement with the droop's key behaviors not only for GaInN LEDs but also for AlGaInP LEDs.

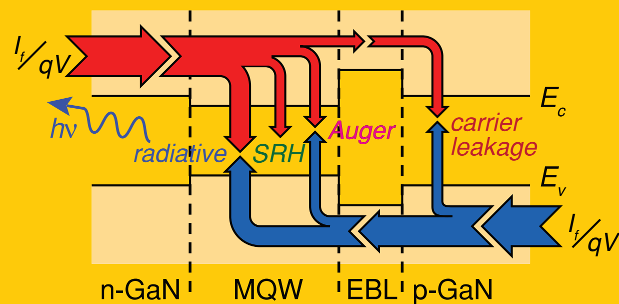

Efficiency droop in light-emitting diodes: Challenges and countermeasures

Jaehee Cho[1], E. Fred Schubert[1], and Jong Kyu Kim[2,*]

1. Introduction

Light-emitting diodes (LEDs) are used in a very broad range of applications, from displaying information, sensing, communications, to lighting and illumination. LEDs are emitters capable of very high efficiency; for example, an LED, in principle, can generate white light with a 20 times greater efficiency than a conventional incandescent light source with a tungsten filament [1,2]. Deployed on a global scale to replace conventional light sources, such solid-state light emitters will result in enormous energy savings, substantial financial savings, and reduction in the emission of global-warming-causing CO_2, acid-rain-causing SO_2, and polluting mercury. GaN-based blue LEDs, as one of the core components, are particularly attractive for illumination applications, because blue LEDs can be combined with phosphors to make a white light source.

One of the most significant and enduring challenges facing high-power GaN-based LEDs is the *efficiency droop* – the decrease in external quantum efficiency (EQE) of an LED with increasing drive current [3]. Typical GaN-based LEDs have a peak in efficiency, typically at current densities less than 10 A/cm^2, above which the efficiency gradually decreases. As shown in Fig. 1, although a GaInN blue LED has a high efficiency at low currents, it can suffer more than 40% loss of efficiency at a higher current, e.g. the desired operating current. The efficiency droop is a particularly severe problem for high-power LEDs which operate at current densities far beyond the point where the efficiency peaks, thus it constitutes a fundamental obstacle for widespread adoption of solid-state lighting. The fundamental cause of the efficiency droop is a topic of active research, and in the opinion of the authors of this article, has been solved. Indeed, we will describe in this article a useful framework that allows for the understanding of the efficiency droop and the implementation of countermeasures that are suited to reduce the efficiency droop.

Let us first explain what the meaning of "solving the efficiency droop" is. Figure 2 shows four efficiency-versus-current curves indicating several solutions, unwanted and wanted. By increasing the area of the LED chip, the current density is reduced, and thus, the peak efficiency is shifted to higher currents, as shown in Fig. 2(a). However, larger devices may suffer from a lower chip yield from a wafer and a scaling penalty, i.e. a decrease in light-extraction efficiency with increasing device area. Typically, LEDs with low peak efficiency due to some reasons such as high defect density, are known to show a small efficiency droop, as shown in Fig. 2(b). In this unwanted case, radiative recombination is not the largest among the recombination mechanisms, thus, it is suppressed by some other non-radiative processes, resulting in the lack of a pronounced peak in efficiency. Figure 2(c) shows a reduced efficiency droop with lower peak efficiency, with the efficiency peak shifted to higher currents.

[1] Future Chips Constellation, Department of Electrical, Computer, and Systems Engineering, Rensselaer Polytechnic Institute, Troy, New York 12180, USA
[2] Department of Materials Science and Engineering, Pohang University of Science and Technology, Pohang 790–784, Korea
*Corresponding author(s): e-mail: kimjk@postech.ac.kr

WILEY ONLINE LIBRARY

© 2012 by WILEY-VCH Verlag GmbH & Co. KGaA, Weinheim

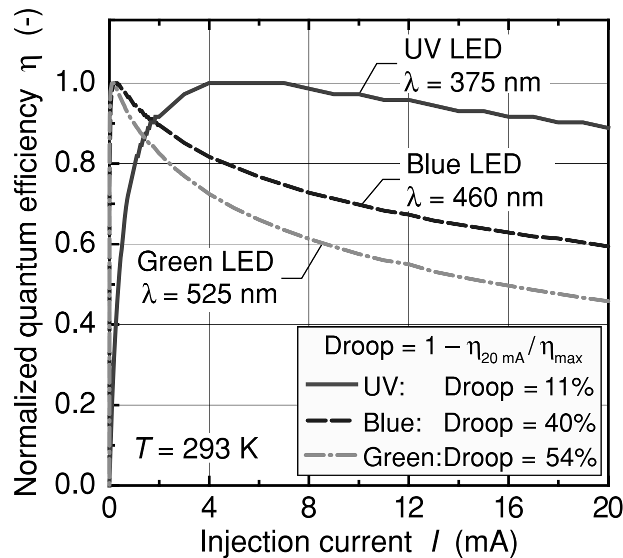

Figure 1 (online color at: www.lpr-journal.org) Efficiency versus current curves of GaN-based UV, blue and green LEDs showing a decrease in efficiency with increasing injection current. The illustration shows that green LEDs have largest efficiency droop.

The above mentioned two cases (b) and (c) are undesirable solutions because they sacrifice low-current efficiency of the device to reduce the efficiency droop. The best solution to be pursued is a decrease of efficiency droop without any loss of low-current efficiency, as shown in Fig. 2(d).

In this article, several proposed explanations for the physical origin of efficiency droop including dislocations, carrier delocalization, Auger recombination, poor hole-injection, and electron leakage from the active region are discussed. For a better understanding of the latter phenomenon, a drift-leakage model is developed to quantitatively explain carrier leakage-out from the active region which is mediated by the asymmetry of the pn junction of LEDs. In addition, possible solutions to overcome efficiency droop are discussed.

2. Current understanding of the efficiency droop mechanism

In this section, we summarize and discuss several mechanisms which are proposed to be responsible for the efficiency droop. Efficiency droop is caused by a non-radiative carrier loss mechanism that has little effect at low currents, but becomes dominant at high currents. In general, carrier losses can occur either inside or outside the active region's quantum wells (QWs). Defect-related Shockley-Read-Hall (SRH) recombination and Auger recombination are non-radiative recombination processes inside the QWs, whereas carrier leakage results in non-radiative recombination outside the QWs. These three non-radiative recombination mechanisms together with radiative recombination are schematically illustrated in Fig. 3. The importance of solving efficiency droop problem has motivated substantial efforts to understand and mitigate the physical mechanism. Several different mechanisms have been proposed so far which will be discussed in the following subsections.

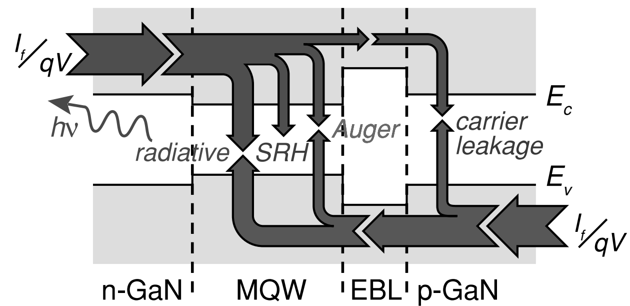

Figure 3 (online color at: www.lpr-journal.org) Schematic illustration of the three non-radiative recombination mechanisms and the radiative recombination mechanism.

2.1. Defect-related mechanisms

Defect-related contributions to efficiency droop have been extensively discussed since point defects and threading dislocations exist in very high concentrations in present GaN-based LEDs. The non-radiative recombination of carriers caused by crystal defects is typically described by the SRH model. However, in simulations based on the conventional SRH scheme, the SRH process unlikely causes the droop at high current injection, although it has a strong influence on the maximum efficiency [4–6]. A number of studies claimed that threading dislocation density is strongly related to efficiency droop based on their comparison

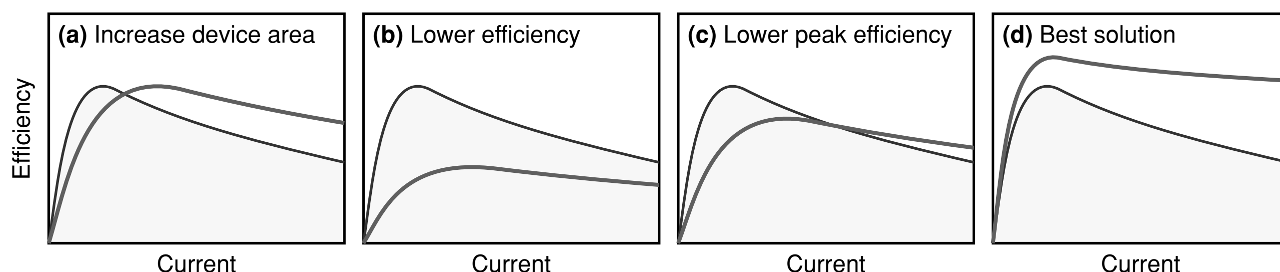

Figure 2 (online color at: www.lpr-journal.org) Efficiency-versus-current curves indicating possible solutions to the efficiency droop.

© 2012 by WILEY-VCH Verlag GmbH & Co. KGaA, Weinheim

between GaInN LEDs grown on sapphire and free-standing GaN substrates [7, 8]; it has been proposed that the lower the threading dislocation density, the lower the efficiency droop. Liu et al. [7] suggested that threading dislocations introduce a number of acceptor-like levels lying within the band gap through which defect-assisted Auger recombination occurs. Bochkareva et al. [9] proposed that the reduction of the injection efficiency by an excess tunneling current from the QW through deep defect states in barriers can be the dominant droop mechanism in their single QW LEDs. It has been reported that a high density of deep levels exists at the core of screw dislocations, and a large concentration of point defects is aggregated in threading dislocations in GaN, which could be the cause of a parasitic non-radiative carrier transport mechanism. Therefore, the carriers can propagate by tunneling between spatially close defect levels formed by such dislocations [10–13]. Schubert et al. [14] analyzed GaInN LEDs grown on templates with low and high threading dislocation densities. The analysis revealed that the low-dislocation-density sample is characterized by a pronounced peak in the efficiency at relatively low currents followed by a rapid decrease in efficiency, whereas the high-dislocation-density sample showed very little decrease in efficiency, but also exhibited a low peak efficiency. The observed behavior was explained in terms of competition between the recombination mechanisms: In the low-defect-density sample, efficiency peaks as radiative recombination overtakes non-radiative recombination before the droop-causing mechanism becomes significant. Then, as the current increases further, the droop-causing mechanism becomes dominant, leading to a reduction in efficiency. In the high-defect-density sample, decreased non-radiative lifetime leads to non-radiative recombination that is larger than radiative recombination even beyond the point where the droop-causing mechanism becomes dominant. Thus, in the high-defect-density sample, radiative recombination never becomes the dominant recombination mechanism, which very well explains the lower peak efficiency and absence of a significant efficiency droop. Despite these differences, however, the form of the droop-causing mechanism was found to be quite similar for the two samples, indicating that threading dislocations are not responsible for the efficiency droop observed in GaInN/GaN LEDs. Photoluminescence (PL) experiments carried out by Shen et al. [15] similarly led to the conclusion that the droop-causing high-current loss mechanism is not affected by the dislocation density.

Dislocations are closely related to one of commonly proposed droop-causing mechanisms: *delocalization of carriers* [10, 16–21]. According to this explanation, electrons and holes are confined to localized potential minima within the QW plane; the potential minima can be caused by fluctuations in QW thickness or indium composition, or by potential barriers surrounding the SRH defects. Carriers within the wells are assumed to be physically separated from dislocations and have long non-radiative lifetimes. For low currents, the injected carrier concentration is small and carriers remain confined to the potential minima, where they recombine with high radiative efficiency. As the current increases, however, the localized potential minima are gradually filled up and carriers are released (delocalized) to the dislocation sites, which leads to greater interaction with non-radiative centers, shorter non-radiative lifetime, and lower efficiency. Hader and colleagues [20, 21] proposed such density-activated defect recombination (DADR) mechanism wherein the loss rate is negligible below a certain threshold carrier density, then it quadratically rises according to the quadratic dependence of the electron-electron scattering rates on the carrier concentration. It has also been suggested that delocalized carriers are more susceptible to parasitic tunneling currents associated with threading dislocations which cause local heating, increasing with the injection, and hence, facilitating the tunneling process typically assisted by acoustic phonons [10]. The dependence of efficiency droop upon indium mole fraction in GaInN QWs has been used to support the above explanation. Yang et al. [19] reported that as the indium composition x in $Ga_{1-x}In_xN$ increases ($x = 0.01$–0.02 for ultraviolet, 0.09 for violet, 0.17 for blue, to 0.30 for green LEDs), the efficiency droop becomes more severe, as shown in Fig. 1, because compositional indium fluctuations typically increase with indium mole fraction. Hammersley et al. [22] supported the carrier-delocalization explanation based on temperature-dependent PL measurements from a GaInN/GaN QW structure.

2.2. Auger recombination

One of the most controversial mechanisms proposed to lead to efficiency droop in GaInN/GaN LEDs is *Auger recombination*. In the Auger process, an electron recombines with a hole, transferring the released energy for exciting a third carrier rather than emitting a photon. In general, the rate of Auger recombination is proportional to the cube of free carrier density. Depending upon the magnitude of the Auger coefficient C, then, it is clear that Auger recombination can drive down the efficiency as the current increases. It is reported that only Auger coefficients greater than 10^{-31} cm^6 s^{-1} can cause significant efficiency droop, therefore, estimation of correct value of Auger coefficient is important [3].

Shen et al. [15] performed PL lifetime studies with resonant optical excitation on thick pseudo-bulk double-heterostructure (DH) GaInN layers with emission wavelengths around 440 nm, and estimated an Auger coefficient in the range of $1.4 \times 10^{-30} \sim 2.0 \times 10^{-30}$ cm^6 s^{-1} from the recombination rate model. Since resonant optical excitation ensures equal generation of electrons and holes in the QWs (and thus simplifies the carrier dynamics compared to electroluminescence which involves the carrier transport) it has become a popular approach to investigate the efficiency droop. Many measurements have been performed on single QW, multiple QWs (MQW), and DH devices [23–29], which were summarized by Piprek [3]. Seemingly conflicting results have been reported, however, as some of references show no decrease in PL efficiency with increasing intensity [24, 26], while others do [15, 25, 29].

© 2012 by WILEY-VCH Verlag GmbH & Co. KGaA, Weinheim

Note that the measurements of the Auger coefficient based on the recombination rate equation, i.e. ABC model – *we will discuss the details on this equation in Section 3* – neglect the effect of carrier leakage. One common assumption made for resonant excitation experiments is that the escape rates for electrons and holes from GaInN QWs are both equal to zero, and that carrier transport-related effects can be neglected. However, Schubert et al. [30, 31] have shown that carriers do escape from the QWs, even under resonant-optical excitation, which raises questions on the ability of resonant excitation experiments to accurately assess the radiative efficiency of GaInN QWs. David and Gardner [32] presented a counter-argument that the use of resonant excitation PL experiments is valid to characterize droop because the carrier leakage during the PL measurement is only significant at low excitation densities (where bands are tilted) but does not contribute to the droop at high excitation densities (where bands are flat). More recently, David and Grundmann [33] performed differential carrier life time measurements to show that the data can be more reliable when phase-space filling is included, and concluded that droop is caused by a shortening of the non-radiative lifetime at high current density which is in quantitative agreement with Auger scattering. In addition, they pointed out that the transport-related effects such as carrier leakage over the active region would not influence the lifetime of trapped carriers in the QWs, thus cannot account for their lifetime reduction observation.

The experimental results described above have motivated several theoretical efforts directed at uncovering the role of Auger recombination in GaInN LEDs. Hader et al. [34] reported a very small Auger coefficient of $C = 3.5 \times 10^{-34}$ cm^6 s^{-1} for the direct band-to-band Auger losses in GaInN QWs based on calculations using fully microscopic many-body models. The same group also investigated other relevant Auger processes such as phonon-assisted Auger recombination [35]. Kioupakis et al. [36] performed atomistic first-principle calculations and proposed that droop is caused by indirect Auger recombination, mediated by electron-phonon coupling and alloy scattering. Delaney et al. [37] reported that interband Auger recombination can be significant in GaInN due to the proximity of a higher-level conduction band; using first-principles density-functional and many-body perturbation theory, they found that the Auger coefficient for bulk GaInN strongly depends upon the bandgap, with a maximum value of around 2×10^{-30} cm^6 s^{-1} when the bandgap of GaInN is around 2.5 eV which corresponds to 500 nm emission. However, the interband Auger coefficient decreases very rapidly when the bandgap deviates from 2.5 eV, while the efficiency droop is observed in a wide range of emission energies. Bertazzi et al. [38] reported much smaller Auger coefficients ($<10^{-32}$ cm^6 s^{-1} with a peak near the bandgap of 2.9 eV) than the coefficients reported in Ref [37], and concluded that the resonant enhancement associated with interband transitions for blue to green wavelengths cannot account for experimentally observed efficiency droop in GaInN-based LEDs. Based on Bertazzi's argument, the interpolation of matrix elements used in Ref [37] may not correctly describe the symmetry of the involved states and thus may not be suitable for the calculation of Auger coefficient in GaInN; this could explain the large difference in the Auger coefficients calculated by the two research groups.

In addition, it has been claimed that good agreement between measured characteristics of GaInN/GaN LEDs and drift-diffusion device models has been achieved using Auger coefficients between 3.5×10^{-31} and 2.5×10^{-30} cm^6 s^{-1} [23, 25], while the rate equation models have been found to agree less well [26, 39]. Recently, Guo et al. [40] reported measured Auger coefficients of 6.1×10^{-32} cm^6 s^{-1} for defect-free GaInN nanowires and 4.1×10^{-33} cm^6 s^{-1} for GaInN/GaN dot-in-nanowire grown on (001) silicon by plasma-assisted molecular beam epitaxy, and no efficiency droop up to an injection current density of 400 A/cm^2.

2.3. Electron leakage

The flow of energetic electrons flying over the active region (without being captured) to recombine with holes in p-type GaN or at the p-type contact electrode, i.e. *electron leakage*, is known as a common problem in GaN-based LEDs and it is the reason why an AlGaN electron-blocking layer (EBL) is implemented on the p-side of the active region. However, the EBL in GaN-based LEDs is often unable to completely block election leakage; for this reason, electron leakage has been suggested as an explanation for efficiency droop. Electron leakage over the EBL can cause the droop only when the leakage current rises stronger with the carrier density than the radiative recombination current [3]. Thus, the band offset ratio, $\Delta E_C/\Delta E_V$, is an important parameter in numerical LED simulations since electron leakage presumably is sensitive to the barrier height, ΔE_C.

Direct experimental proof of electron leakage beyond the EBL was recently provided: Vampola et al. [41] experimentally confirmed the occurrence of electron leakage in an LED test structure with a short-wavelength QW embedded in the p-type region. The short-wavelength emission appeared at currents just before the efficiency reached its peak value, and then intensified as the current increased further and the EQE decreased, indicating a direct connection between the efficiency droop and electron leakage. Chang et al. [42] carried out a similar experiment, and suggested that the occurrence of electron leakage significantly decreases the peak EQE and shifts the starting point of efficiency droop to a higher current density. In addition, temperature-dependent electroluminescence measurements have provided clues which suggest that electron leakage can be the dominant droop-causing mechanism [43–45]. Recently, Nguyen et al. [46] demonstrated that the maximum achievable quantum efficiency of GaN-based dot-in-a-wire LEDs is limited by electron leakage rather than Auger recombination. They demonstrated a phosphor-free white GaN-based nanowire LED with a p-doped AlGaN EBL.

© 2012 by WILEY-VCH Verlag GmbH & Co. KGaA, Weinheim

The LED exhibited virtually zero efficiency droop for injection currents up to 2200 A/cm^2; the authors proposed that electron leakage is the primary mechanism for droop in the GaN-based nanowire LED.

"Electron leakage" serves as an umbrella term which actually encompasses several distinct problems or phenomena that result in the flow of carriers through the active region without recombining. Among these are: (i) a poor hole-injection efficiency; (ii) an ineffective EBL; (iii) an incomplete capture of electrons by QWs; and (iv) electron escape from the QWs. Necessarily, therefore, fewer holes than electrons are injected into the active region. These two phenomena – escape of electrons form the active region and poor hole injection – are components of any carrier leakage explanation for efficiency droop. However, because it is not obvious which is cause and which is effect, both have been proposed. Hole injection into the active region may be the limiting factor, possibly due to low p-type doping efficiency, low hole mobility caused by large effective hole mass, and the EBL acting as a potential barrier also for holes. As a result of the low hole injection, current across the device is dominated by electrons. The alternative explanation is that the MQW active region and EBL structure inadequately confines electrons to the active region, and that the electrons escape to the p-type side where they recombine non-radiatively with holes, before the holes ever have the chance to enter the active region. While these two explanations are related, the course of action needed to correct carrier leakage in these two cases is actually quite different: For example, if poor hole-injection efficiency is to blame, decreasing the bandgap of the EBL – which acts as a barrier to hole injection – or p-type doping of the active region would be advisable. However, if insufficient confinement of electrons is to blame, then increasing the bandgap of the EBL or modification of the MQW active region based on a polarization engineering technique would be advisable. The following subsections discuss limited hole-injection efficiency, ineffective EBL, and incomplete capture of carriers by quantum wells in detail.

2.3.1. Poor hole-injection efficiency

Although the EBL is intended to confine electrons to the active region, it also has an effect on the transport of holes. The valence band offset of AlGaN relative to GaN results in a barrier for holes. This barrier is reduced by incorporation of p-type doping in the AlGaN layer; however, p-type doping efficiency decreases as the Al mole fraction increases [47–49]. As a result, increasing Al content in the EBL to more strongly confine electrons will simultaneously make it more difficult for holes to enter the active region. The effects of increasing Al content in AlGaN EBLs – increased difficulty of hole injection and greater electron confinement – make it difficult to ascertain whether electron leakage is or is not successfully suppressed. Hole injection is further hindered as compared to electron injection due to the fact that active regions are typically intrinsic (undoped) or n-type doped. Note that the problem of limited hole transport is independent of material polarization and sheet charges at hetero-interfaces; therefore, this mechanism can be expected to be relevant even in LEDs grown in non-polar and semi-polar orientations or polarization-matched LEDs grown on c-plane sapphire. Recently, Hwang et al. [50] introduced a new device named light-emitting triodes which have two anodes for promoting the injection of holes into the active region, and showed that limited hole-injection efficiency is one of the dominant mechanisms responsible for the efficiency droop.

2.3.2. Ineffective EBL

Electron and hole transport characteristics in GaN-based devices are known to be vastly different. Electrons typically have fairly high mobilities of 200 cm^2 V^{-1} s^{-1} or more, and high concentrations are achievable due to the relatively low ionization energy of the n-type dopant Si [51]. By contrast, the ionization energy of the p-type dopant Mg is around 170 meV, and therefore, high hole concentrations are difficult to achieve [48,52]. In addition, holes in GaN have a lower mobility, with values on the order of 10 cm^2 V^{-1} s^{-1} being typical [47].

For maximum efficiency, the goal is to have equal numbers of electrons and holes injected into the active region. However, higher electron concentrations and mobilities favor electron transport, and therefore virtually all GaInN/GaN LEDs include large-bandgap p-type AlGaN EBLs intended to prevent electrons from escaping to the p-type region; Al mole fractions in the EBL are typically close to 15%. However, while an EBL with Al content in this range may be optimal, it is not clear that such an EBL is actually sufficient to completely confine electrons, since increasing the Al content to raise the barrier for electrons also increases polarization mismatch with respect to GaN. For LED structures grown in the c-direction, this polarization discontinuity results in sheet charges at hetero-interfaces [53].

Figure 4(a) shows the calculated energy-band diagram of a conventional GaInN/GaN MQW LED at a forward current of 350 mA. Due to differences in spontaneous and piezoelectric polarization between layers in the MQW and the EBL, positive and negative sheet charges are generated, which strongly affect the energy-band diagram. At the interface between the GaN QB or spacer and AlGaN EBL, as shown in Fig. 4(b), there exists a positive sheet charge which is attractive to electrons. As a result, the conduction band of the EBL is pulled down, which reduces the effective barrier height for electrons. As this sheet charge increases with rising Al content, the conduction band edge is pulled down further, which results in a barrier height increase that is smaller than the increase in conduction band offset between the EBL and GaN. Therefore, even as the Al content is increased, complete confinement of electrons to the active region may not be possible. The combination of these effects allows for a significant electron leakage current as much as 60% of the total current [24].

© 2012 by WILEY-VCH Verlag GmbH & Co. KGaA, Weinheim

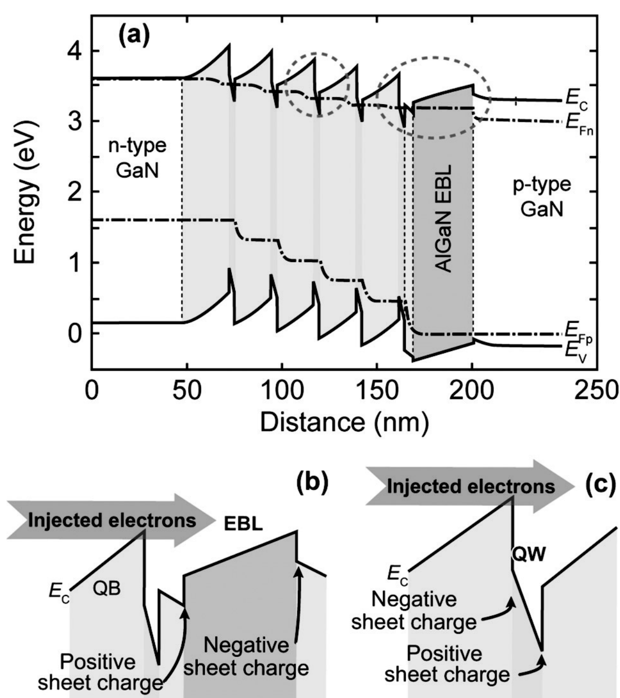

Figure 4 (online color at: www.lpr-journal.org) (a) Calculated energy band diagram of a typical GaInN/GaN MQW LED (area 1 $\times$ 1 mm^2) at an injection current level of 350 mA. Schematic energy-band diagram (b) near the EBL, and (c) near a QW with consideration of sheet charges.

2.3.3. Incomplete carrier capture by QWs and carrier escape from QWs

Electrons and holes located in a barrier preceding a QW may be coherently transported across or reflected from the QW, may be captured into the QW by emitting one or more optical phonons, or may be captured by the QW through acoustic-phonon-mediated or impurity-mediated scattering events [54]. Only those carriers captured by a QW are able to participate in radiative recombination and contribute to the optical power produced by an LED. GaInN/GaN QWs grown along the c-direction have distinct characteristics which can affect the capture of carriers [55]. As shown in Fig. 4(c), electrons injected from the n-type region face large triangular barriers, which result from the mismatch in polarization in the GaInN QW and GaN QB. Inside the QW is a large electric field, which means that the conduction band edge of the barrier on the n-type side of the QW (injection barrier) is higher in energy than the band edge of the barrier on the p-type side of the QW (extraction barrier). Holes injected from the p-type region similarly face triangular barriers.

The effect of polarization charges and QW width upon capture has also been analyzed in terms of the quantum-mechanical dwell time (the time an electron dwells over the QW), which is related to the probability of carrier capture [55]. It was shown that the presence of sheet charges results in decreased carrier-capture probability and dwell time; eliminating or inverting the charges would result in substantially longer dwell times. Further, increasing the QW thickness also increases the dwell time, and therefore should lead to a higher capture probability.

The impact of sheet charges at the QW interfaces also appears in simple drift-diffusion LED models which do not specifically consider carrier capture. In such models, all carriers incident upon a QW are assumed to be captured, and any electron leakage is the result of escape. As shown in Fig. 4(c), the sheet charges resulting from polarization mismatch create barriers for injection; they also lower the barrier for carriers to escape. The interface between QW and barrier on the p-type side features a positive sheet, which is attractive to electrons and lowers the conduction band edge. The interface between QW and barrier on the n-type side features a negative sheet charge, which attracts holes and raises the valence band edge. The cumulative effect of the charges and the resultant modifications of the band diagram are to enable a leakage current that accounts for a substantial fraction of the total current [24]. The occurrence of carrier escape has also been verified experimentally using optical excitation [30,31]. A numerical study using a drift-diffusion model of the effect of polarization upon carrier leakage and the efficiency of GaInN LEDs was performed by Kim et al. [24]. Good agreement was achieved between measured LED characteristics and the simulated results, in which Auger recombination was not included. Droop was observed in the simulated efficiency curve due to carrier leakage out of the active region that increased with current. A similar agreement between measurements and simulations that implicate carrier leakage as the origin of droop was also found by Xie et al. [26].

Although several theories have been employed in this section to explain the origin of efficiency droop, a general consensus among researchers has remained elusive, and seemingly conflicting data have been presented. Nevertheless, there have been successful efforts to reduce or overcome efficiency droop in GaN-based LEDs grown on c-plane sapphire substrates, which include: (i) reducing the carrier density by employment of wide QWs or LED chips with large area [56, 57], (ii) reducing the electron leakage by modification of MQW structures [58–67] and EBL structures [68–72], and (iii) polarization-engineered MQW and EBL structures [24, 53, 55, 73–83]. LEDs grown in the m-plane, a-plane, and other non-polar or semi-polar planes of the wurtzite crystal have been topics of active research to reduce efficiency droop [84–89]. These designs inherently have a lower polarization mismatch than the conventional *c*-plane polar LEDs that are universal in industry. Recently, Zhao et al., reported a high-power LED homoepitaxially grown on free-standing semipolar (20–2–1) GaN substrate with a high external quantum efficiency of 45.3% and very small droop of 14.3% at 200 A/cm^2 [85]. However, homoepitaxial growth along nonpolar and semipolar directions is challenging, and very high quality bulk GaN substrates must be used to achieve significant emission efficiency. These native GaN substrates are expensive and typically very small in area, which makes homoepitaxially grown nonpolar or semipolar LEDs currently

 © 2012 by WILEY-VCH Verlag GmbH & Co. KGaA, Weinheim

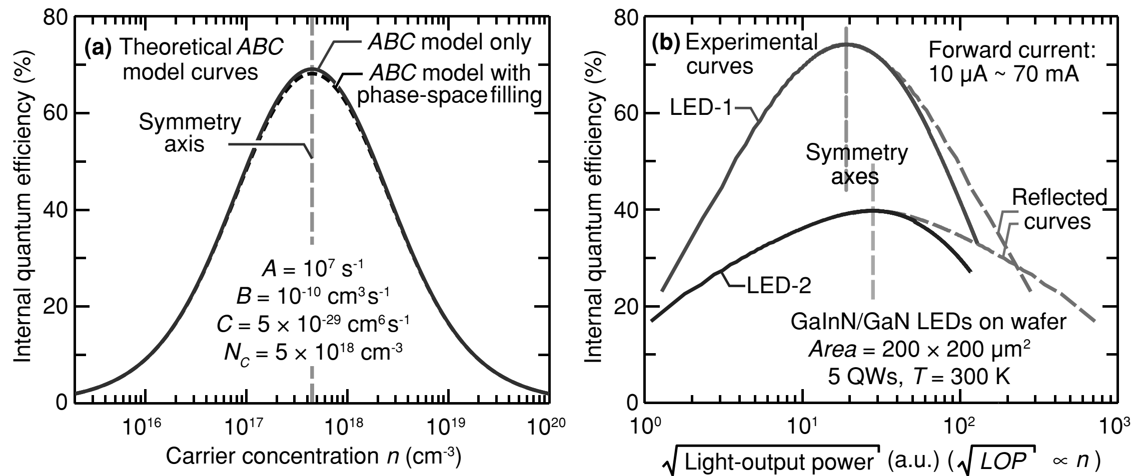

Figure 5 (online color at: www.lpr-journal.org) (a) Theoretical IQE-versus-n curves based on the ABC model (without and with phase-space filling) showing even symmetry with respect to the peak-efficiency point. (b) Experimental IQE-versus-Square root (LOP) curves showing asymmetry.

unfeasible for the general illumination application. No efficiency droop up to an injection current density of 400 A/cm^2 was observed for defect-free GaInN nanowires and GaInN/GaN dot-in-nanowire samples grown on (001) silicon by plasma-assisted molecular beam epitaxy [40]. The absence of droop was attributed to a suppressed defect-assisted Auger recombination process due to the very small measured Auger coefficients.

3. Recombination rate equation and drift-leakage model

In order to better understand the physical mechanisms inside an LED, the carrier recombination rate, R, has been analyzed by means of $\mathrm{A}n + \mathrm{B}n^2 + \mathrm{C}n^3$, where n, A, B, and C represent carrier concentration, SRH, radiative recombination, and Auger recombination coefficient, respectively. The reason that this model – often referred to as the 'ABC model' – has been widely used in discussions of the efficiency droop is that the ABC model is believed to reveal the cause when expressing the internal quantum efficiency (IQE) as IQE $= \mathrm{B}n^2/R$ [4]. However, the IQE of an LED should be expressed as the product of the radiative efficiency (RE) in the active region, which is RE $= \mathrm{B}n^2/R$, and the injection efficiency (IE); that is IQE = RE × IE. The injection efficiency can be limited by non-capture of carriers into the active region as well as leakage of carriers out of the active region [55]. Therefore, it was found that plotting the LED EQE against carrier density exposes this fundamental limitation of the ABC model: The ABC model alone is unsuited to take into account a less-than-100% injection efficiency. A fundamental deficiency in the ABC model used to describe carrier behavior in an LED was observed and reported in Ref. [4]: The ABC model expresses that carriers undergo one of three recombination processes: SRH recombination, a non-radiative process that is proportional to the carrier density; radiative recombination, which is proportional to the square of the carrier density; and Auger recombination, a non-radiative recombination process that depends on the cube of the carrier density. One of the inherent properties of the ABC model is that any plot of LED efficiency (i.e. EQE) as a function of carrier density (plotted on a log scale) should be symmetric with respect to the peak-efficiency point, as shown in Fig. 5(a). However, experimental measurement data does not display this symmetry. For this reason, Dai et al. [4] concluded that the ABC model is insufficient for describing a droop phenomenon. When measuring the efficiency of two different MQW devices, plots of LED efficiency as a function of the square root of light-output power showed that the ABC model cannot account for the behavior of these LEDs, as shown in Fig. 5(b). Although a good fit can be obtained for the efficiency curve at carrier densities below that of the LED peak efficiency, the model fails to keep pace with the decline in efficiency at higher carrier densities. Thus the experiment showed that at high current densities, there is a significant loss process that depends on the carrier density according to a power series with higher-than-third-order terms of the carrier density. The higher order terms suggest an additional process not included in the three conventional processes of the ABC model. The additional process was attributed to carrier leakage.

Based on this knowledge, the '$ABC + f(\mathrm{n})$ model' has been developed and used to analyze the carrier recombination mechanism in LEDs with the equation $R = \mathrm{A}n + \mathrm{B}n^2 + \mathrm{C}n^3 + f(n)$, where $f(n)$ represents carrier leakage out of the active region [90]. This equation can describe all possible recombination processes in an LED. The term $f(n)$ can be expanded into a power series and may have higher-than-third-order contributions to the recombination. The total third-order non-radiative coefficient (which may include an $f(n)$ leakage contribution and an Auger contribution)

© 2012 by WILEY-VCH Verlag GmbH & Co. KGaA, Weinheim

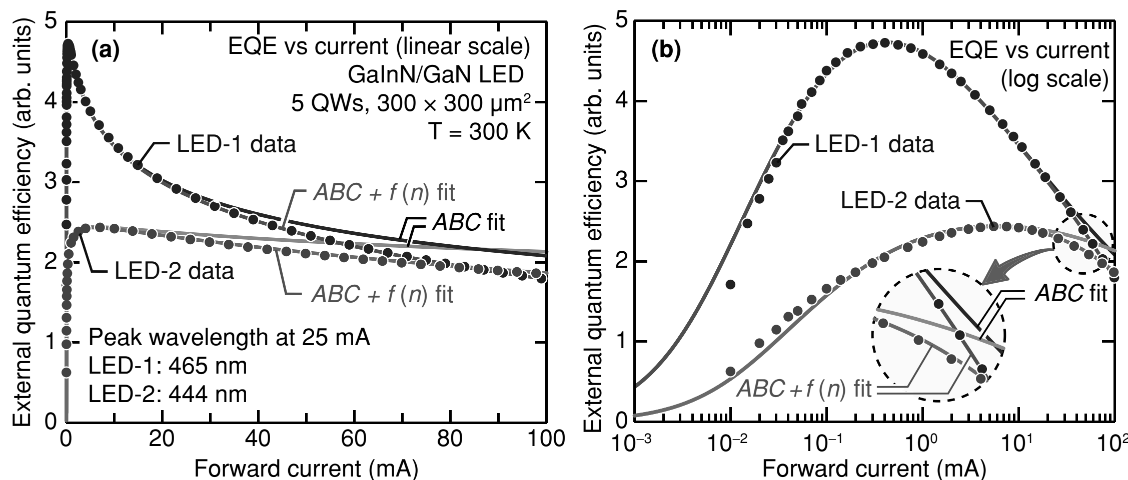

Figure 6 (online color at: www.lpr-journal.org) EQE versus current and theoretical *ABC* model and *ABC* + *f* (*n*) model fits (a) on linear, and (b) logarithmic current scale for two LEDs. Whereas the *ABC* + *f* (*n*) model gives an excellent fit, the *ABC* model deviates from experimental results particularly at high currents, as shown in the inset.

was found to be 8×10^{-29} cm^6 s^{-1} [90]. This large third-order non-radiative coefficient determined by experiment and fitting is so large that it only can be explained by adding the term $f(n)$ to ABC model. Comparison of the theoretical $ABC + f(n)$ model with experimental data shows that a good fit requires the inclusion of the $f(n)$ term, particularly at high current densities, as shown in Fig. 6.

Let us think further about the ABC + f(n) model to find a physical meaning of f(n). To do this, the efficiency droop is analyzed in the framework of carrier leakage driven by the asymmetry in carrier transport characteristics, i.e., there is a significant disparity between electron and hole concentrations as well as mobilities such that $n \gg p$ and $\mu_n \gg \mu_p$. This framework is indeed fulfilled in the AlGaInP and the AlGaInN material system [91]. Based on Shockley's pn junction theory, it is known that the carrier concentration injected into the neutral regions increases with applied forward voltage. Under low-level injection conditions, the current has an exponential relationship with applied bias. The low-level injection condition can be expressed by the following inequality $\Delta n_p(0) \ll p_{p0}$, where $\Delta n_p(0)$ is the injected electron concentration at the edge of the p-type neutral region of a pn junction. When this condition is broken, high-level injection occurs, and both drift and diffusion currents in the p-type region must be considered [92]. An important consideration, however, is the conductivity in each region of the device. When the conductivity in the depletion region becomes comparable to conductivity of the p-side, the series resistance of the p-type layer begins to play a role. Therefore, the low-level condition should be generalized to include the effect of carrier mobility:

$$\mu_n \Delta n_p(0) \ll \mu_p p_{p0} \tag{1}$$

When this generalized condition is broken, the depletion region is flooded with electrons and its resistivity becomes smaller than that of the p-type region. As a result, an electric field will develop in the p-type neutral region as the voltage applied to the diode increases. Furthermore, in the case of extreme high-level injection, i.e. when $\Delta n_p(0) \approx p_{p0}$, the electron-drift current at the edge of the p-type neutral region (where $n = p$) is higher by a factor of μ_n/μ_p than the hole drift current. The difference can exceed a factor of 10 for AlGaInP and GaInN semiconductors, which makes these material systems particularly prone to enter into the high-level injection regime.

Next, a quantitative condition for the onset of electron drift in the p-type region of LEDs is derived using GaInN as an exemplary material system. Given that, in a GaInN LED, the thickness of p-type GaN cladding layer typically is smaller than the electron minority carrier diffusion length, the electron diffusion current leaking out of the active region of a heterojunction LED can be expressed as [91]

$$J_{\text{diffiusion}} = \frac{eD_n \Delta n_p(0)}{L_{\text{p-layer}}} \tag{2}$$

where $L_{\text{p-layer}}$ is the thickness of the p-type GaN, e is the elementary charge, and D_n is the electron diffusion coefficient in the p-type GaN. As the diode enters high-level injection, some of the applied voltage starts to drop across the low-conductivity p-type layer and a drift current arises. The drift current of electrons injected into the p-type neutral layer, at the edge of the neutral layer, is given by

$$J_{\text{drift}} = e\mu_n \Delta n_p(0) E = eD_n \frac{e}{kT} \Delta n_p(0) \frac{J_{\text{total}}}{\sigma_p} \tag{3}$$

where we employed the Einstein relation, and E, J_{total}, and σ_p, are the electric field in the p-type layer, the total current density of the diode, and the p-type layer conductivity ($\sigma_p = e\, p_{p0}\, \mu_p$), respectively. The drift-induced leakage current increases with the total current, and will, at a sufficiently large current, become significant. As a consequence, the injection efficiency into the active region is

© 2012 by WILEY-VCH Verlag GmbH & Co. KGaA, Weinheim

reduced and the device enters the droop regime. It was shown that the onset of the efficiency droop in GaInN LEDs indeed occurs in the high-level injection regime where an electric field emerges in the p-type GaN layer [93].

The total recombination rate in an LED device can be described by the equation, $R = An_{QW} + Bn_{QW}^2 + f(n_{QW})$, where $f(n_{QW})$ is a general loss term causing the efficiency droop [90, 94] and includes drift-induced reduction in injection efficiency (drift leakage), as well as Auger recombination ($C_{Auger}\ n_{QW}{}^3$). Next, the carrier-concentration dependence of diffusion- and drift-leakage current densities is analyzed. The diffusion-leakage current density has the following dependence on carrier concentration

$$J_{diffusion} = \frac{eD_n}{L_{p\text{-layer}}} \Delta n_p(0) = \frac{eD_n}{L_{p\text{-layer}}} \delta n_{QW} \tag{4}$$

where $\delta = \Delta n_p(0)/n_{QW}$ is estimated to be on the order of 0.1% [95]. Close to the peak-efficiency point, where radiative recombination dominates, the recombination rate can be approximated by $R \approx Bn_{QW}^2$. In this region, the total current density, J_{total}, depends on the carrier concentration in the QW according to

$$J_{total} = ed_{active} R \approx ed_{active} Bn_{QW}^2 \tag{5}$$

where d_{active} is the active-region thickness. Inserting Eq. (5) into Eq. (3), we find the following dependence of the drift-induced leakage-current on carrier concentration

$$J_{drift} = e\mu_n \delta n_{QW} \frac{J_{total}}{e\mu_p p_{p0}} \approx ed_{active} \frac{\delta \mu_n}{\mu_p p_{p0}} Bn_{QW}^3 = ed_{active} C_{DL} n_{QW}^3 \tag{6}$$

where C_{DL} is a proportionality constant associated with the lowering of the injection efficiency due to drift of electrons in the p-type layer ("drift leakage"). Since the $f(n_{QW}) \propto n_{QW}^3$ dependence (drift-induced leakage, see Eq. 6) is stronger than the $f(n_{QW}) \propto n_{QW}$ dependence (diffusion-induced leakage, see Eq. 4), the latter one may be neglected. Writing $f(n) = C_{DL} n_{QW}^3 + D_{DL} n_{QW}^4 + \cdots$ allows one to identify the third-order coefficient as

$$C_{DL} = \frac{\delta \mu_n}{\mu_p\ p_{p0}} B \tag{7}$$

As a numerical example, we choose: $p_{p0} = 5.0 \times 10^{17}$ cm^{-3}, $\mu_p = 2.5$ cm^2/(Vs), $\mu_n = 300$ cm^2/(Vs), $B = 10^{-10}$ cm^3/s, and $\delta = 0.1\%$. Using these values, we obtain $C_{DL} = 2.4 \times 10^{-29}$ cm^6/s, in agreement with experimental values [3, 39].

At even higher current densities, when the drift-induced leakage current becomes significant, the dependence of the total current density, J_{total}, shifts from a $J_{total} \propto n_{QW}^2$ dependence to a $J_{total} \propto n_{QW}^3$ dependence, i.e.,

$$J_{total} = e\, d_{active} R \approx ed_{active}\, C_{DL}\, n_{QW}^3 \tag{8}$$

and consequently, the dominant term of the loss function $f(n_{QW})$ shifts from $f(n_{QW}) \propto n_{QW}^3$ to $f(n_{QW}) \propto n_{QW}^4$. Inserting Eq. (8) into Eq. (3) yields

$$J_{drift} = e\mu_n \delta n_{QW} \frac{J_{total}}{e\mu_p p_{p0}} \approx ed_{active} \left(\frac{\delta \mu_n}{\mu_p p_{p0}}\right)^2 Bn_{QW}^4 = ed_{active}\, D_{DL}\, n_{QW}^4 \tag{9}$$

The equation allows one to identify the fourth-order coefficient as

$$D_{DL} = \left(\frac{\delta \mu_n}{\mu_p p_{p0}}\right)^2 B \tag{10}$$

A fourth-power dependence of $f(n)$ has indeed been reported in the literature [4]. The total recombination rate can then be written as

$$R = An_{QW} + Bn_{QW}^2 + f(n_{QW}) = An_{QW} + Bn_{QW}^2 + C_{Auger}\, n_{QW}^3 + C_{DL} n_{QW}^3 + D_{DL} n_{QW}^4 \tag{11}$$

where both drift-induced reduction of the injection efficiency as well as Auger losses are included. The quantities involved in Eqs. (7) and (10) are known to be strongly temperature-dependent. It is well known that p_{p0} decreases exponentially with decreasing temperature while the temperature-dependent mobilities of electrons and holes, which are not necessarily monotonic, are more complicated. Qualitatively, the p_{p0} term is expected to dominate the temperature dependence of Eqs. (7) and (10). Therefore, we predict that the C_{DL} and D_{DL} coefficients will increase with decreasing temperature, leading to an increased droop.

The analytic model developed here is worthy of notice because the drift-induced leakage function $f(n)$ is shown to have a 3rd-order as well as a 4th-order dependence on the carrier concentration; furthermore, electron drift in the p-type layer (and its dependence on carrier density) causes a decrease of the injection efficiency and an associated reduction in IQE, i.e. the efficiency droop. Based on the analytic model presented here, the current density at which the efficiency reaches its peak value, i.e., the onset-of-droop current density can be calculated. The carrier concentration, at which the efficiency reaches its maximum, n_{peak}, can be expressed as $n_{peak} = \sqrt{A_{SRH}/C}$ [4]. Near the peak efficiency, the total recombination rate R is dominated by Bn^2. Therefore, based on the drift-induced leakage model, the onset-of-droop current density can be expressed as

$$J_{onset\text{-}of\text{-}droop} = ed_{active} Bn_{peak}^2 = ed_{active} \frac{BA}{C_{DL}} = ed_{active} A \frac{p_{p0}\mu_p}{\delta \mu_n} \tag{12}$$

As a numerical example, we use the parameters $d_{active} = 3.0$ nm, $A_{SRH} = 1.0 \times 10^7$ /s, $p_{p0} = 5.0 \times 10^{17}$ cm^{-3},

© 2012 by WILEY-VCH Verlag GmbH & Co. KGaA, Weinheim

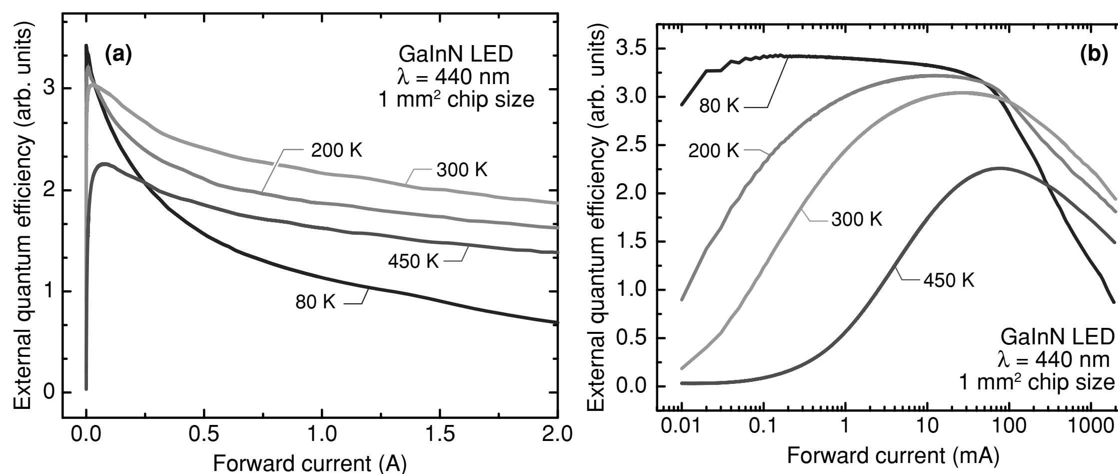

Figure 7 (online color at: www.lpr-journal.org) Measured EQE of a GaInN LED for several temperatures ranging from 80 K to 450 K using (a) linear and (b) logarithmic abscissa.

$\mu_p = 2.5\ \text{cm}^2/(\text{Vs})$, $\mu_n = 300\ \text{cm}^2/(\text{Vs})$, and $\delta = 0.1\%$. Using these values in the above equation, an onset-of-droop current density of 2.0 A/cm^2 is calculated. This value is within the range of experimental onset-of-droop current densities, which typically are between 1.0 and 10 A/cm^2 [93, 96, 97].

4. Droop analysis in GaInN and AlGaInP LEDs based on the drift-leakage model

In this section, we will discuss experimental results on the efficiency droop in high-quality GaInN LEDs and AlGaInP LEDs. As for the GaInN LEDs, they are grown by metalorganic vapor phase epitaxy and have five GaInN/GaN QWs which emit at a peak wavelength of 440 nm. The LED structure employs an $Al_{0.15}Ga_{0.85}N$ EBL and a p-type GaN after the MQW growth on n-type GaN. Thin-film LEDs are fabricated by bonding the LED wafer to a silicon wafer and utilizing laser-lift-off to remove the sapphire substrate. The measured samples are diced into $1 \times 1\ \text{mm}^2$ chips that are left unpackaged. A chip is mounted with thermal grease in a liquid-nitrogen-cooled cryostat. By cooling the LEDs to near liquid N_2 temperatures (about 77 K), hole freeze-out can be enhanced, leading to a very asymmetric junction (i.e. $n \gg p$). The light-output power is then measured as a function of temperature using pulsed operating conditions with a 5 μs pulse-duration and a 1% duty ratio.

Figure 7 shows the measured EQE vs. current at several different temperatures with (a) linear and (b) logarithmic abscissa. One of the noticeable features is that the LED shows the largest efficiency droop at 80 K. As the temperature increases to 200 K, the efficiency droop is reduced, but still greater than the droop observed at room temperature, 300 K. We believe that this behavior can be well explained by the asymmetry in the transport properties of electrons and holes (including the temperature dependence), which is discussed in the previous section. As the temperature decreases, fewer acceptors are ionized. This leads to a larger asymmetry in carrier concentration, and therefore an onset of high-level injection conditions at lower currents. At the lowest temperature 80 K, the onset of droop occurs at the smallest current density. A few trends are apparent from these curves: at low temperatures, the peak efficiency point is higher and occurs at a smaller current density. This agrees with expectations that SRH recombination is minimized at low temperatures [91, 94]. Therefore, it can be proposed that the onset of high-level injection results in the buildup of an electric field in the p-type region resulting in stronger electron leakage and a shift of the recombination location into the p-side. As the temperature increases, the concentration of available holes increases so that the onset of high-level injection occurs at higher current, resulting in less electron spillover and less series resistance.

Let us move on to discuss experimental results on high-quality AlGaInP LEDs based on the same argument. First of all, the following characteristics of the AlGaInP material system are noteworthy: (1) AlGaInP/AlInP heterostructure LEDs homo-epitaxially grown on GaAs substrates are lattice matched, and thus have a negligibly small threading dislocation density. (2) The QWs in the active region of the AlGaInP LEDs are numerous and the individual QWs are slightly thicker (about 4.0 nm) when compared to typical GaInN QWs (about 3.0 nm). (3) AlGaInP/AlInP/GaAs heterostructures are not subject to spontaneous and piezoelectric polarization electric fields. These three characteristics are in marked contrast to the GaInN/GaN material system [91]. The AlGaInP LEDs used in this study have a multiple quantum well active region consisting of 38 pairs of $(Al_xGa_{1-x})_{0.5}In_{0.5}P$ QWs and AlInP QBs, and a $350 \times 350\ \mu\text{m}^2$ chip size. The emission wavelength of the LED is about 630 nm at room temperature. Considering this emission wavelength, it is not close to

© 2012 by WILEY-VCH Verlag GmbH & Co. KGaA, Weinheim

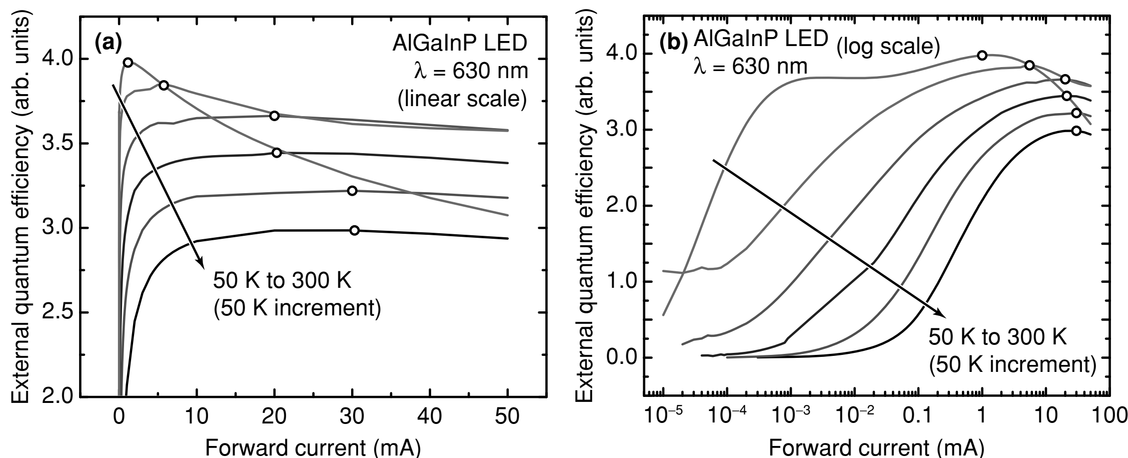

Figure 8 (online color at: www.lpr-journal.org) EQE vs. current of an AlGaInP LED for different temperatures using (a) linear and (b) logarithmic abscissa. Open black circles indicate the peak position of each curve.

direct-indirect bandgap transition of AlGaInP material system (the direct-indirect bandgap transition occurs at about 532 nm).

Figure 8 shows the EQE of the red AlGaInP LED as a function of current at different temperatures with (a) linear and (b) logarithmic abscissa. By inspecting Fig. 8(a), we can recognize the following trends: First, as the temperature increases, the magnitude of the peak efficiency decreases, due to increased SRH non-radiative recombination. Second, because SRH recombination increases with temperature, the peak efficiency point also shifts to higher currents at high temperature. Third, the magnitude of the efficiency droop increases with decreasing temperature and is largest at 50 K. As a temperature increases to 100 K, the efficiency droop is reduced, but still significantly larger than at room temperature. Note that similar droop behavior with respect to temperature has been discussed previously for the GaInN/GaN material system. Given the similarity of the measured EQE vs. current curves, it is likely that the droop in GaInN LEDs and in AlGaInP LEDs has the same physical origin. One similarity of both material systems is the asymmetry of electron and hole concentration and mobility. As the temperature decreases in the AlGaInP LED, acceptor ionization, which is very efficient at room temperature, begins to decline. This effect may cause the observed trends in the efficiency droop. Furthermore, the temperature dependence of $J_{\text{onset-of-droop}}$, i.e. a decreasing $J_{\text{onset-of-droop}}$ with decreasing T, is due to the strong dependence of p_{p0} on T (see Eq. 12). It may be noted that while the GaInN system has a low hole concentration and mobility, the AlGaInP system also has a low hole concentration and mobility (although not as problematic as GaInN). In fact, this is the reason that the efficiency droop in AlGaInP material system becomes apparent only at lower temperature (about 100 K) in contrast to the droop in GaInN material system which occurs at room temperature. This similarity of the material properties can explain the occurrence of droop in these two material systems.

The results presented here for GaInN and AlGaInP LEDs may shed light on other mechanisms that have been proposed to cause efficiency droop as discussed in Section 2. It is known that AlGaInP-based alloy semiconductors do not suffer from an excessive composition fluctuation. This lack of excessive compositional fluctuations is supported by the spectrally narrow emission lines that are found for this material system (not shown here). Furthermore, AlGaInP LEDs are homo-epitaxially grown on GaAs substrates so that the dislocation density is negligibly small. Therefore, it is doubtful that the efficiency droop in AlGaInP LEDs could be attributed to a carrier-delocalization effect and enhanced recombination at dislocations, which was proposed for the GaInN materials system. In addition, with respect to polarization fields on the efficiency droop, they likely compound the problem of electron leakage, making it easier for electrons to escape the MQW region [24, 98]. However, spontaneous and piezo-electric polarization-field effects are absent in the AlGaInP/AlInP/GaAs material system. For this reason, polarization effects cannot be the primary or fundamental cause of the efficiency droop in AlGaInP LEDs. Furthermore, since the QWs in the AlGaInP LEDs are relatively thick, and the number of QWs is large, Auger recombination is not expected to be a significant effect in AlGaInP LEDs. Furthermore, the absence of droop at room temperature and the presence of the droop at cryogenic temperatures suggest that the droop-causing mechanism becomes stronger at low temperatures. This temperature dependence is contrary to what is expected from Auger recombination (i.e., it is a high-carrier-concentration phenomenon that would not be expected to increase at low temperatures). We point out again that the asymmetry of a pn junction made of III-V semiconductors can be exacerbated at low temperatures: acceptor ionization energies are generally higher than donor ionization energies. Results show that significant droop occurs when the asymmetry intentionally is exacerbated. Therefore, we conclude that the asymmetry in

© 2012 by WILEY-VCH Verlag GmbH & Co. KGaA, Weinheim

carrier transport properties of the pn junction is the dominant cause of the efficiency droop in both nitride- and phosphide-based LEDs. This result is very plausible considering the previously-mentioned discussion of Section 2.

5. Conclusion

We present a summary of the current state of efficiency droop research and review mechanisms potentially causing the droop. It seems the LED community has not yet reached a consensus on the answer to the question "what mechanism is actually responsible for droop" and further experiments and much time will likely be needed to fully resolve the issue. An analytic model is developed for understanding the efficiency droop in LEDs made from semiconductors having strong asymmetry in carrier concentration and mobility. Under high-injection conditions, electron drift in the p-type layer of the diode causes a decrease of the injection efficiency. As the conductivity of electrons leaking out of the MQW approaches the conductivity of holes on the p-side, the low-level injection condition is broken leading to an electric field in the p-side cladding layer of the junction that further enhances leakage and droop. The drift-induced leakage is shown to have a 3rd and 4th power dependence on the carrier concentration in the active region. The model is suited to explain experimental efficiency-versus-current curves of both nitride- and phosphide-based LEDs. Experimental evidence is presented that is consistent with the asymmetry of a pn junction, specifically the large disparity in carrier concentration and mobility, causing the efficiency droop in GaInN and even AlGaInP LEDs. Based on the attribution of the efficiency droop to the strong asymmetry of carrier-transport properties of the LEDs, the improvement of p-type conductivity (both p and μ_p) is considered a key factor in the reduction and potential solution of the efficiency droop.

Acknowledgements. J.C. and E.F.S. would like to thank Dr. Q. Dai, D. Meyaard, G.-B. Lin, and Dr. J.-I. Shim for fruitful discussions. Authors J.C. and E.F.S. were supported by Sandia's Solid-State Lighting Sciences Center, an Energy Frontier Research Center funded by the U.S. Department of Energy, US National Science Foundation, Office of Basic Energy Sciences, Samsung Electronics, and Magnolia Optical Technologies, Inc. Author J. K. Kim gratefully acknowledge support by the Industrial Technology Development Program and International Collaborative R&D Program funded by Korean Ministry of Knowledge Economy, Priority Research Centers funded by National Research Foundation of Korea (2010–0029711), Global Research Network program (2011–220-D00064), Ministry of Education, Science and Technology of Korea, and POS-LED Center by POSCO and Seoul Semiconductor.

Received: 7 May 2012, **Revised:** 12 August 2012,
Accepted: 14 September 2012

Published online: 26 December 2012

Key words: Light-emitting diode, efficiency droop, compound semiconductor, carrier asymmetry.

Jaehee Cho is a senior research scientist in the Future Chips Constellation at Rensselaer Polytechnic Institute (RPI), USA. He earned his PhD degree in materials science and engineering from the Seoul National University, Korea. He worked as a senior research scientist at the Samsung Advanced Institute of Technology, Korea, for 10 years until he joined RPI in 2008. Cho's research interests have been in the areas of device fabrication and optical/electrical analysis of light-emitting diodes, laser diodes, and photovoltaics.

E. Fred Schubert made pioneering contributions to the field of compound semiconductor materials and devices, particularly to the doping of compound semiconductors and to the development and understanding of light-emitting diodes. He is currently a distinguished professor at Rensselaer Polytechnic Institute in Troy, NY. He authored the books *Doping in III–V Semiconductors* (1992), *Delta Doping of Semiconductors* (1996), and *Light-Emitting Diodes* (1st edition 2003 and 2nd edition 2006). He is a Fellow of the APS, IEEE, OSA, and SPIE and has received several awards.

Jong Kyu Kim is an assistant professor at the Department of Materials Science and Engineering in POSTECH. After he received his PhD degree from POSTECH in 2002, he joined the Future Chips Constellation at Rensselaer Polytechnic Institute as a research assistant professor. Dr. Kim has made pioneering contributions to the field of GaN-based LEDs and nano-structured thin film materials by oblique-angle deposition technique and their applications. He is a member of Materials Research Society (MRS), the Minerals, Metals & Materials Society (TMS), and the International Society for Optical Engineering (SPIE).

References

[1] E. F. Schubert and J. K. Kim, Science **308**, 1274 (2005).
[2] M. R. Krames, O. B. Shchekin, R. Mueller-Mach, G. O. Mueller, L. Zhou, G. Harbers, and M. G. Craford, J. Disp. Technol. **3**, 160 (2007).
[3] J. Piprek, Phys. Status Solidi A **207**, 2217 (2010).
[4] Q. Dai, Q. Shan, J. Cho, E. F. Schubert, M. H. Crawford, D. D. Koleske, M.-H. Kim, and Y. Park, Appl. Phys. Lett. **98**, 033506 (2011).
[5] I. V. Rozhansky and D. A. Zakheim, Semiconductors **40**, 839–845 (2006).
[6] K. A. Bulashevich, V. F. Mymrin, S. Yu. Karpov, I. A. Zhmakin, and A. I. Zhmakin, J. Comput. Phys. **213**, 214 (2006).

© 2012 by WILEY-VCH Verlag GmbH & Co. KGaA, Weinheim

[7] Z. Liu, T. Wei, E. Guo, X. Yi, L. Wang, J. Wang, G. Wang, Y. Shi, I. Ferguson, and J. Li, Appl. Phys. Lett. **99**, 091104 (2011).
[8] K. Akita, T. Kyono, Y. Yoshizumi, H. Kitabayashi, and K. Katayama, J. Appl. Phys. **101**, 033104 (2007).
[9] N. I. Bochkareva, V. V. Voronenkov, R. I. Gorbunov, A. S. Zubrilov, Y. S. Lelikov, P. E. Latyshev, Y. T. Rebane, A. I. Tsyuk, and Y. G. Shreter, Appl. Phys. Lett. **96**, 133502 (2010).
[10] B. Monemar and B. E. Semelius, Appl. Phys. Lett. **91**, 181103 (2007).
[11] J. W. P. Hsu, M. J. Manfra, S. N. G. Chu, C. H. Chen, L. N. Pfeiffer, and R. J. Molnar, Appl. Phys. Lett. **78**, 3980 (2001).
[12] E. Müller, D. Gerthsen, P. Brückner, F. Scholz, Th. Gruber, and A. Wagg, Phys. Rev. B **73**, 245316 (2006).
[13] W. J. Ha, S. Chhajed, S. J. Oh, S. Hwang, J. K. Kim, J.-H. Lee, and K.-S. Kim, Appl. Phys. Lett. **100**, 132104 (2012).
[14] M. F. Schubert, S. Chhajed, J. K. Kim, E. F. Schubert, D. D. Koleske, M. H. Crawford, S. R. Lee, A. J. Fischer, G. Thaler, and M. A. Banas, Appl. Phys. Lett. **91**, 231114 (2007).
[15] Y. C. Shen, G. O. Müller, S. Watanabe, N. F. Gardner, A. Munkholm, and M. R. Krames, Appl. Phys. Lett. **91**, 141101 (2007).
[16] S. Chichibu, T. Azuhata, T. Sota, S. Nakamura, Appl. Phys. Lett. **69**, 4188 (1996).
[17] A. Y. Kim, W. Gotz, D. A. Steigerwald, J. J. Wierer, N. F. Gardner, J. Sun, S. A. Stockman, P. S. Martin, M. R. Krames, R. S. Kern, and F. M. Steranka, Phys. Status Solidi A **188**, 15 (2001).
[18] B. Monemar and B. E. Sernelius, Appl. Phys. Lett. **91**, 181103 (2007).
[19] Y. Yang, X. A. Cao, and C. Yan, IEEE Trans. Elect. Dev. **55**, 1771 (2008).
[20] J. Hader, J. V. Moloney, and S. W. Koch, Appl. Phys. Lett. **92**, 221106 (2010).
[21] J. Hader, J. V. Moloney, and S. W. Koch, Appl. Phys. Lett. **99**, 181127 (2011).
[22] S. Hammersley, T. J. Badcock, D. Watson-Parris, M. J. Godfrey, P. Dawson, M. J. Kappers, and C. J. Humphreys, Phys. Status Solidi C **8**, 2194 (2011).
[23] K. A. Bulashevich and S. Yu. Karpov, Phys. Status Solidi C **5**, 2066 (2008).
[24] M. H. Kim, M. F. Schubert, Q. Dai, J. K. Kim, E. F. Schubert, J. Piprek, and Y. Park, Appl. Phys. Lett. **91**, 183507 (2007).
[25] A. Laubsch, M. Sabathil, W. Bergbauer, M. Strassburg, H. Lugauer, M. Peter, S. Lutgen, N. Linder, K. Streubel, J. Hader, J. V. Moloney, B. Pasenow, and S. W. Koch, Phys. Status Solidi C **6**, S913 (2009).
[26] J. Xie, X. Ni, Q. Fan, R. Shimada, Ü. Özgür, and H. Morkoç, Appl. Phys. Lett. **93**, 121107 (2008).
[27] M. Meneghini, N. Trivellin, G. Meneghesso, E. Zanoni, U. Zehnder, and B. Hahn, J. Appl. Phys. **106**, 114508 (2009).
[28] M. Zhang, P. Bhattacharya, J. Singh, and J. Hinckely, Appl. Phys. Lett. **95**, 201108 (2009).
[29] A. Laubsch, M. Sabathil, J. Baur, M. Peter, and B. Hahn, IEEE Trans. Elect. Dev. **57**, 79 (2010).
[30] M. F. Schubert, J. Xu, Q. Dai, F. W. Mont, J. K. Kim, and E. F. Schubert, Appl. Phys. Lett. **94**, 081114 (2009).
[31] M. F. Schubert, Q. Dai, J. Xu, J. K. Kim, and E. F. Schubert, Appl. Phys. Lett. **95**, 191105 (2009).
[32] A. David and N. F. Gardner, Appl. Phys. Lett. **97**, 13508 (2010).
[33] A. David and M. Grundmann, Appl. Phys. Lett. **96**, 103504 (2010).
[34] J. Hader, J. V. Moloney, B. Pasenow, S. W. Koch, M. Sabathil, N. Linder, and S. Lutgen, Appl. Phys. Lett. **92**, 261103 (2008).
[35] B. Pasenow, S. W. Koch, J. Hader, J. V. Moloney, M. Sabathil, N. Linder, and S. Lutgen, Phys. Status Solidi C **6**, S864 (2009).
[36] E. Kioupakis, P. Rinke, K. T. Delaney, and C. G. Van de Walle, Appl. Phys. Lett. **98**, 161107 (2011).
[37] K. T. Delaney, P. Rinke, and C. G. Van de Walle, Appl. Phys. Lett. **94**, 191109 (2009).
[38] F. Bertazzi, M. Goano, and E. Bellotti, Appl. Phys. Lett. **97**, 231118 (2010).
[39] H.-Y. Ryu, H.-S. Kim, and J.-I. Shim, Appl. Phys. Lett. **95**, 081114 (2009).
[40] W. Guo, M. Zhang, P. Bhattacharya, and J. Heo, Nano Lett. **11**, 1434 (2011).
[41] K. J. Vampola, M. Iza, S. Keller, S. P. DenBaars, and S. Nakanura, Appl. Phys. Lett. **94**, 061116 (2009).
[42] L.-B. Chang, M.-J. Lai, R.-M. Lin, and C.-H. Huang, Appl. Phys. Express **4**, 012106 (2011).
[43] C. H. Wang, J. R. Chen, C. H. Chiu, H. C. Kuo, Y.-L. Li, T. C. Lu, and S. C. Wang, IEEE Photon. Technol. Lett. **22**, 236 (2010).
[44] K. Fujiwara, H. Jimi, and K. Kaneda, Phys. Status Solidi C **6**, S814 (2009).
[45] J. Wang, L. Wang, W. Zhao, Z. Hao, and Y. Luo, Appl. Phys. Lett. **97**, 201112 (2010).
[46] H. P. T. Nguyen, K. Cui, S. Zhang, M. Djavid, A. Korinek, G. A. Botton, and Z. Mi, Nano Lett. **12**, 1317 (2012).
[47] U. Kaufmann, P. Schlotter, H. Obloh, K. Köhler, and M. Maier, Phys. Rev. B **62**, 10867 (2000).
[48] K. B. Nam, M. K. Nakarmi, J. Li, J. Y. Lin, and H. X. Jiang, Appl. Phys. Lett. **83**, 878 (2003).
[49] A. Khan, K. Balakrishnan, and T. Katona, Nature Photon. **2**, 77 (2008).
[50] S. Hwang, W. J. Ha, J. K. Kim, J. Xu, J. Cho, and E. F. Schubert, Appl. Phys. Lett. **99**, 181115 (2011).
[51] W. Götz, N. M. Johnson, C. Chen, H. Liu, C. Kuo, and W. Imler, Appl. Phys. Lett. **68**, 3144 (1996).
[52] V. Bougrov, M. E. Levinshtein, S. L. Rumyantsev, and A. Zubrilov, in Properties of Advanced Semiconductor Materials: GaN, AlN, InN, BN, SiC, SiGe. edited by M. E. Levinshtein, S. L. Rumyantsev, and M. S. Shur (Wiley, New York, 2001).
[53] J. Xu, M. F. Schubert, D. Zhu, J. Cho, E. F. Schubert, H. Shim, and C. Sone, Appl. Phys. Lett. **99**, 041105 (2011).
[54] D. Bradt, Y. M. Sirenko, and V. Mitin, Semicond. Sci. Technol. **10**, 260 (1995).
[55] M. F. Schubert and E. F. Schubert, Appl. Phys. Lett. **96**, 131102 (2010).
[56] M. Maier, K. Köhler, M. Kunzer, W. Pletschen, and J. Wagner, Appl. Phys. Lett. **94**, 041103 (2009).
[57] D. A. Zakheim, A. S. Pavluchenko, and D. A. Bauman, Phys. Status Solidi C **8**, 2340 (2011).

© 2012 by WILEY-VCH Verlag GmbH & Co. KGaA, Weinheim

[58] P.-M. Tu, C.-Y. Chang, S.-C. Huang, C.-H. Chiu, J.-R. Chang, W.-T. Chang, D.-S. Wuu, H.-W. Zan, C.-C. Lin, H.-C. Kuo, and C.-P. Hsu, Appl. Phys. Lett. **98**, 211107 (2011).
[59] C. S. Xia, Z. M. S. Li, W. Lu, Z. H. Zhang, Y. Sheng, and L. W. Cheng, Appl. Phys. Lett. **99**, 233501 (2011).
[60] Y.-K. Kuo, M.-C. Tsai, S.-H. Yen, T.-C. Hsu, and Y.-J. Shen, IEEE J. Quantum Electron. **46**, 1214 (2010).
[61] Y.-Y. Zhang, G.-H. Fan, Y.-A. Yin, and G.-R. Yao, Opt. Express **20**, A133 (2012).
[62] J.-Y. Chang, M.-C. Tsai, and Y.-K. Kuo, Opt. Lett. **35**, 1368 (2010).
[63] C. H. Wang, S. P. Chang, W. T. Chang, J. C. Li, Y. S. Lu, Z. Y. Li, H. C. Yang, H. C. Kuo, T. C. Lu, and S. C. Wang, Appl. Phys. Lett. **97**, 181101 (2011).
[64] C. H. Wang, S. P. Chang, P. H. Ku, J. C. Li, Y. P. La, C. C. Lin, H. C. Yang, H. C. Kuo, T. C. Lu, S. C. Wang, and C. Y. Chang, Appl. Phys. Lett. **99**, 171106 (2011).
[65] Y.-J. Lee, C.-H. Chen, and C.-J. Lee, IEEE Photonic. Tech. Lett. **22**, 1506 (2010).
[66] M.-C. Tsai, S.-H. Yen, Y.-C. Lu, and Y.-K. Kuo, IEEE Photonic. Tech. Lett. **23**, 76 (2011).
[67] S.-H. Han, D.-Y. Lee, H.-W. Shim, G.-C. Kim, Y. S. Kim, S.-T. Kim, S.-J. Lee, C.-Y. Cho, and S.-J. Park, J. Phys. D: Appl. Phys. **43**, 354004 (2010).
[68] R.-M. Lin, M.-J. Lai, L.-B. Chang, and C.-H. Huang, Appl. Phys. Lett. **97**, 181108 (2010).
[69] S.-H. Yen, M.-C. Tsai, M.-L. Tsai, Y.-J. Shen, T.-C. Hsu, and Y.-K. Kuo, IEEE Photonic. Tech. Lett. **21**, 975 (2009).
[70] C. H. Wang, C. C. Ke, C. Y. Lee, S. P. Chang, W. T. Chang, J. C. Li, Z. Y. Li, H. C. Yang, H. C. Kuo, T. C. Lu, and S. C. Wang, Appl. Phys. Lett. **97**, 261103 (2010).
[71] Y. Y. Zhang and Y. A. Yin, Appl, Phys. Lett. **99**, 221103 (2011).
[72] Y. Y. Zhang and G.-R. Yao, Appl. Phys. Lett. **110**, 093104 (2011).
[73] J. H. Son and J.-L. Lee, Appl. Phys. Lett. **97**, 032109 (2010).
[74] Y. B. Tao, Z. Z. Chen, F. F. Zhang, C. Y. Jia, S. L. Qi, T. J. Yu, X. N. Kang, Z. J. Yang, L. P. You, D. P. Yu, and G. Y. Zhang, J. Appl. Phys. **107**, 103529 (2010).
[75] J. H. Son and J.-L. Lee, Opt. Express **18**, 5466 (2010).
[76] Y.-K. Kuo, J.-Y. Chang, and M.-C. Tsai, Opt. Lett. **35**, 3285 (2010).
[77] M. L. Reed, E. D. Readinger, C. G. Moe, H. Shen, M. Wraback, A. Syrkin, A. Usikov, O. V. Kovalenkov, and V. A. Dmitriev, Phys. Status Solidi C **6**, 585 (2009).
[78] M.-H. Kim, W. Lee, D. Zhu, M. F. Schubert, J. K. Kim, E. F. Schubert, and Y. Park, IEEE J. Sel. Topics Quantum Electron. **15**, 1122 (2009).
[79] H. Song, J. S. Kim, E. K. Kim, Y. G. Seo, and S.-M. Hwang, Nanotechnology **21**, 134026 (2010).
[80] S. P. Chang, T. C. Lu, L. F. Zhuo, C. Y. Jang, D. W. Lin, C. H. Yang, H. C. Kuo, and S. C. Wang, J. Electrochem. Soc. **157**, H501 (2010).
[81] Y.-K. Kuo, J.-Y. Chang, M.-C. Tsai, and S.-H. Yen, Appl. Phys. Lett. **95**, 011116 (2009).
[82] H. J. Chung, R. J. Choi, M. H. Kim, J. W. Han, Y. M. Park, Y. S. Kim, H. S. Paek, C. S. Sone, Y. J. Park, J. K. Kim, and E. F. Schubert, Appl. Phys. Lett. **95**, 241109 (2009).
[83] S. Choi, H. J. Kim, S.-S. Kim, J. Liu, J. Kim, J.-H. Ryou, R. D. Dupuis, A. M. Fischer, and F. A. Ponce, Appl. Phys. Lett. **96**, 221105 (2010).
[84] C.-H. Chiu, D.-W. Lin, C.-C. Lin, Z.-Y. Li, W.-T. Chang, H.-W. Hsu, H.-C. Kuo, T.-C. Lu, S.-C. Wang, W.-T. Liao, T. Tanikawa, Y. Honda, M. Yamaguchi, and N. Sawaki, Appl. Phys. Express **4**, 012105 (2011).
[85] Y. Zhao, S. Tanaka, C.-C. Pan, K. Fujito, D. Feezell, J. S. Speck, S. P. Denbaars, and S. Nakamura, Appl. Phys. Express **4**, 082104 (2011).
[86] X. Li, X. Ni, J. Lee, M. Wu, Ü. Özgür, H. Morkoc, T. Paskova, G. Mulholland, and K. R. Evans, Appl. Phys. Lett. **95**, 121107 (2009).
[87] S.-C. Ling, T.-C. Lu, S.-P. Chang, J.-R. Chen, H.-C. Kuo, and S.-C. Wang, Appl. Phys. Lett. **96**, 231101 (2010).
[88] H. Zhong et al., Appl. Phys. Lett. **90**, 233504 (2007).
[89] M. C. Schmidt, K.-C. Kim, H. Sato, N. Fellows, H. Masui, S. Nakamura, S. P. DenBaars, and J. Speck, Jpn. J. Appl. Phys. **46**, L126 (2007).
[90] Q. Dai, Q. Shan, J. Wang, S. Chhajed, J. Cho, E. F. Schubert, M. H. Crawford, D. D. Koleske, M.-H. Kim, and Y. Park, Appl. Phys. Lett. **97**, 133507 (2010).
[91] E. F. Schubert, Light-Emitting Diodes, 2nd ed. (Cambridge University Press, Cambridge, 2006).
[92] S. M. Sze and K. K. Ng, Physics of Semiconductor Devices, 3rd ed. (Wiley, Hoboken, 2007).
[93] D. S. Meyaard, G.-B. Lin, Q. Shan, J. Cho, E. F. Schubert, H. Shim, M.-H. Kim, and C. Sone, Appl. Phys. Lett. **99**, 251115 (2011).
[94] D. S. Meyaard, Q. Shan, Q. Dai, J. Cho, E. F. Schubert, M.-H. Kim, and C. Sone, Appl. Phys. Lett. **99**, 041112 (2011).
[95] G.-B. Lin, D. Meyaard, J. Cho, E. F. Schubert, H. Shim, and C. Sone, Appl. Phys. Lett. **100**, 161106 (2012).
[96] M. F. Schubert, J. Xu, J. K. Kim, E. F. Schubert, M. H. Kim, S. Yoon, S. M. Lee, C. Sone, T. Sakong, and Y. Park, Appl. Phys. Lett. **93**, 041102 (2008).
[97] Y.-L. Li, Y.-R. Huang, and Y.-H. Lai, Appl. Phys. Lett. **91**, 181113 (2007).
[98] J. Xu, M. F. Schubert, A. N. Noemaun, D. Zhu, J. K. Kim, E. F. Schubert, M. H. Kim, H. J. Chung, S. Yoon, C. Sone, and Y. Park, Appl. Phys. Lett. **94**, 011113 (2009).

© 2012 by WILEY-VCH Verlag GmbH & Co. KGaA, Weinheim